SCIENCE CHINA
Technological Sciences

April 2012 Vol.55 No.4: 1146–1152
doi: 10.1007/s11431-011-4730-4

# Experiment on surface charge distribution of fine sediment

HUANG Lei[1], FANG HongWei[1*] & CHEN MingHong[2]

[1] *Department of Hydraulic Engineering, State Key Laboratory of Hydro-Science and Engineering, Tsinghua University, Beijing 100084, China;*
[2] *College of Water Conservancy and Civil Engineering, China Agricultural University, Beijing 100083, China*

Received May 9, 2011; accepted August 24, 2011; published online February 25, 2012

Surface charge distribution of particles is the fundamental problem for adsorption and desorption between sediment and contaminant. In this paper, we take quartz sand for example to measure its micro-morphology and surface charge distribution using the phase mode of the electrical force microscope. Then the statistical relation of micro-morphology and surface charge distribution is obtained. Results show that quartz sand possesses complex surface morphology, which has great impact on the charge distribution. Positive and negative charges mostly concentrate on the saddle, convex and concave parts of the surface, while distribute less in the groove, ridge and flat parts. This experiment provides a new method for understanding the process of flocculation in coastal and estuarine zone.

**sediment, surface charge, micro-morphology**

**Citation:** Huang L, Fang H W, Chen M H. Experiment on surface charge distribution of fine sediment. Sci China Tech Sci, 2012, 55: 1146–1152, doi: 10.1007/s11431-011-4730-4

## 1 Introduction

Recent years, agricultural non-point source pollution and industrial point source pollution causing river pollution have become increasingly serious with the rapid development of social economy. There are strong physical, chemical and biological interactions between sediment and contaminant. Surface charge distribution of particles is the fundamental problem for adsorption and desorption studies. For colloidal particles, sediment particles and some other particles, there have been many studies about the impact of surface charge properties on adsorption and flocculation, which mostly use the Derjaguin-Landau-Verwey-Overbeek (DLVO) theory in colloidal chemistry. The DLVO theory is an ideal model that assumes the particle is symmetrical sphere with smooth surface and uniform charge distribution. It describes the colloidal stability considering electrostatic force and van der Waals force. However, sediment particle has extremely complex morphology and pores of various scales. Approximating sediment surface with ideal sphere ignores much important information of the particle. Therefore, there are some limitations in explaining interactions between particles and contaminants with DLVO theory.

Quartz sand, an important industrial material, is river sand, sea sand and mountain sand, which contains a large percentage of silica. Because of unique physical and chemical properties, quartz sand plays a vital role in aviation, aerospace, electronic, machinery and other industries. Studies on quartz sand mainly focus on micro-structural anaylsis and adsorption properties. Liu et al. [1–4] have continuously observed quartz particles of Chinese loess, red soil, Chengdu clay and Zhejiang sea sand with scanning electron microscope, and analyzed micro-structure to reveal the transport process and deposition environment. Ren et al. [5] studied adsorption of amino sulfonate amphoteric sur-

*Corresponding author (email: fanghw@mail.tsinghua.edu.cn)

factants on quartz sand. Results showed adsorption process fits Langmuir adsorption isotherm well and temperature rising will cause a significant reduction in platform adsorption capacity. Qu et al. [6, 7] studied the adsorption of thermal recovery additive on quartz sand, and the impact of salt and alcohol, and concluded that salt increases adsorption capacity while alcohol reduces adsorption capacity. In order to enhance the adsorption capacity of quartz sand, researchers modified the surface with iron salts and manganese oxides. Wang et al. [8–10] has done relative research. However, these studies on adsorption remained at macro level and lacked in-depth understanding of microscopic mechanism.

Electrical force microscope (EFM) is a kind of surface analysis technique developed on the basis of atomic force microscope (AFM) over the past decade [11], belonging to the scanning probe microscope (SPM) family. This technology can obtain both surface morphology and charge distribution in nano-scale. Many studies have been carried out on surface charge properties of various materials. Han et al. [12, 13] measured the charge distribution on the surface of polyimide film and chitosan using EFM, respectively. Taboada et al. [14] measured surface charge heterogeneity of a silica plate through measuring a two-dimensional array of force versus distance curves in electrolyte solutions with different ionic strengths and pH values via AFM. Yin et al. [15] measured charge distribution of a multiphase volcanic rock, especially across the boundary between adjacent phases. However, direct measurement of surface charge distribution of sediment has not been reported.

Through mineral composition analysis of sediment along the Yangtze River, we found 50% of the composition is quartz. Therefore, this paper takes quartz sand for example to measure its micro-morphology and surface charge distribution using scanning probe microscope. It will enhance understanding of surface charge distribution for quartz sand, which provides a foundation for its adsorption mechanism study, and prepares for adsorption and flocculation study of natural sediment at micro-level.

## 2 Experiment

Quartz sands with size range of 0.3–0.5 mm were collected from natural rivers, and stored in a clean glass dish. To image the surface morphology and charge distribution, we chose some quartz sand particles with tweezers and stuck them onto metal sample plate with double-sided adhesive. The whole process should be as fast as possible to reduce contamination of the sample. Experiments were completed with DI 3100 Atomic Force Microscope in the Department of Physics at Tsinghua University.

AFM morphology image was obtained in air using contact mode, with scanning range of 5 μm×5 μm, and scanning array of 256×256. All images were obtained in constant force mode. Many samples were prepared and at least three different positions were chosen for observation of each sample. Position selection should be random, which may ensure each position has different characteristics, to enhance its representativeness.

EFM measured surface charge distribution with MESP probe which was coated with a layer of conductive metal film. First, we scanned surface morphology with conductive probe in tapping mode. Avoiding the impact of surface morphology on charge signal, probe was driven back to the original position and elevated 50 nm vertically after morphological characteristic was recorded. Then we turned off the closed-loop feedback system and carried out an open-loop scanning in accordance with recorded surface morphology. This is the lift-mode function of electrical force microscope, which eliminates the impact of surface morphology on charge measurement [16, 17].

Phase image was obtained through charge measurement. Phase image shows the phase angle shift (hereafter referred to as phase shift) between piezoelectric actuator driving signal and actual cantilever oscillation [18–20]. The tip-sample interactions change cantilever's vibrational characteristic and cause resonance phase shift. Phase shift is presented on the screen through the signal acquisition and processing system. Magonov et al. [21] analyzed the effect of tip-sample interactions on cantilever vibration by introducing effective force constant $k_{\text{eff}} = k + \sigma$, and the phase shift of cantilever vibration could be expressed as

$$\Delta\phi_0 \approx \frac{Q\sigma}{k}, \tag{1}$$

where $Q$ represents quality factor; $k$ is the spring constant; $\sigma$ represents the sum of the force derivatives for all the forces $F_i$ acting on the cantilever. We consider only the electrostatic force $F = -k' q_{\text{tip}} q_{\text{surf}} / z^2$, and the sum of the force derivatives $\sigma$ is expressed as

$$\sigma = \sum \frac{\partial F_i}{\partial z} = \frac{2k' q_{\text{tip}} q_{\text{surf}}}{z^3}, \tag{2}$$

where $k'$ is the electrostatic constant; $z$ represents the relative displacement between the tip and sample which is set as a constant; $q_{\text{tip}}$ and $q_{\text{surf}}$ are surface charges of tip and sample. $q_{\text{tip}}$ is constant when the bias voltage on the tip is given. So eq. (1) is rewritten as

$$\Delta\phi_0 \approx \frac{Q}{k} \cdot \frac{2k' q_{\text{tip}} q_{\text{surf}}}{z^3} \propto q_{\text{surf}}. \tag{3}$$

Eq. (3) shows that phase image provides a map of charge distribution on the sample surface. The phase shift is positive when the electrostatic force acting on the tip is repulsive and negative when the force is attractive. Particularly, the greater phase shift, the greater charge density.

## 3 Results and discussion

### 3.1 Surface morphology of quartz sand

Figure 1 is the morphology image of quartz sand obtained by AFM, which shows the morphology characteristic in nano-scale. Brighter regions imply higher elevation. Units of *x*-axis and *y*-axis are both μm, and surface elevation difference is up to 200 nm. Figure 2 is the surface re-construction of quartz sand by MATLAB, with horizontal and vertical coordinates representing pixel array.

AFM image possesses a high resolution. Figure 1 takes a scanning array of 256×256. More scanning points result in higher resolution, and give a more detailed description of sample surface. Compared with the scanning electron microscope (SEM) image [1–4], AFM image not only has a high resolution, but also can directly give the surface height of quartz sand, providing convenience for data analysis.

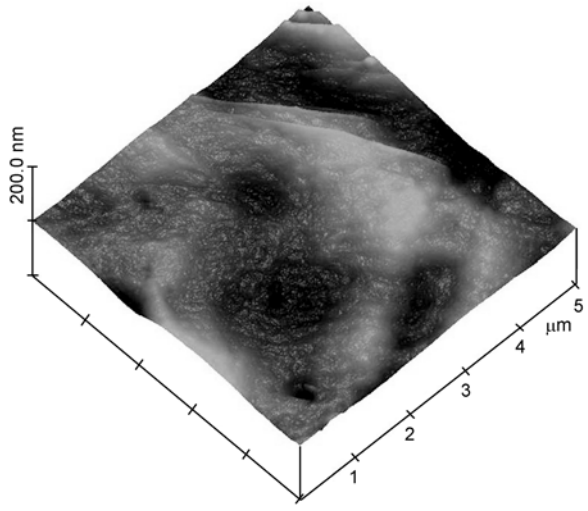


**Figure 1** AFM image of quartz sand.

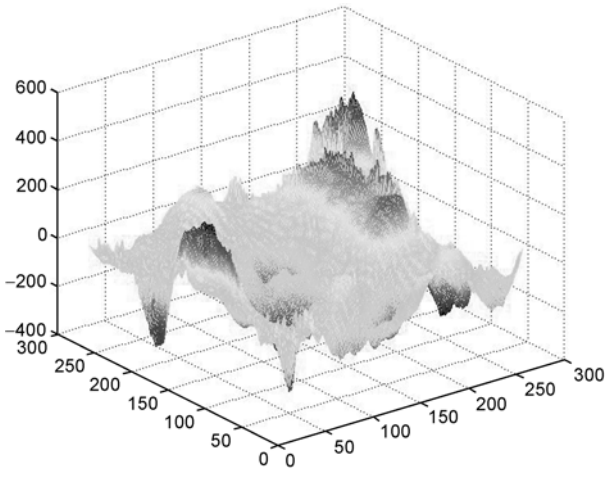


**Figure 2** Surface re-construction of quartz sand.

However, SEM image needs to transform surface gray matrix into a height matrix, which involves optical problems and requires the consistency of surface scattering intensity when obtaining image.

### 3.2 Surface charge distribution of quartz sand

Figure 3 shows the results of EFM measurement, with scanning range of 10 μm×10 μm and scanning array of 256 ×256. The space between different scanning points is about 39 nm, providing a detailed description of surface morphology and charge distribution of quartz sand. The left is the morphology image, in which bright regions and dark regions imply high elevation and low elevation, respectively. The right one is the phase image, where bright regions represent positive phase shift, implying repulsive electrostatic force acting on the tip. In addition, dark regions represent negative phase shift, implying attractive electrostatic force acting on the tip. The sign of phase shift characterizes the sign of charge and the magnitude of phase shift can determine the strength of charge.

The right phase image was obtained when bias voltage of +5 V was added on the conductive tip. As above, the bright regions imply positive phase shift and repulsive force acting on the tip, so charge distributing in these regions should be positive, and brighter regions imply stronger positive charges. In contrast, dark regions imply negative phase shift and attractive force acting on the tip, so the charges there should be negative, and darker regions imply stronger negative charges. Compared with the left morphology image, we can conclude that surface charge distribution has a strong correlation with morphology. Regions with more complex morphology take a greater charge density. When no bias voltage was added on the tip, we got only weak information of charge distribution. When bias voltage of −5 V was added, conclusion was drawn similar to bias voltage of +5 V.

To reflect the statistical properties of surface charge distribution, we plotted the frequency histogram of phase shift, as seen in Figure 4. It shows that phase shift of quartz sand obeys a standard normal distribution. Under bias voltage of +5 V, the mean phase shift is negative (−0.02°), that is attractive force and negatively charged for the overall performance. However, under bias voltage of −5 V, the mean phase shift is positive (+0.008°), that is repulsive force and also negatively charged for the overall performance, which proves the conclusion under bias voltage of +5 V. The standard normal distribution illustrates that both positively charged and negatively charged regions exist on the surface of quartz sand, with an overall performance of weak negative charging.

Further, we chose two cross sections of quartz sand for analysis, as seen in Figure 3. Figure 5 shows the morphology images of cross sections. Figure 6 is the corresponding phase images reflecting the charge distributions of cross sections. During the scanning process with lift-mode of

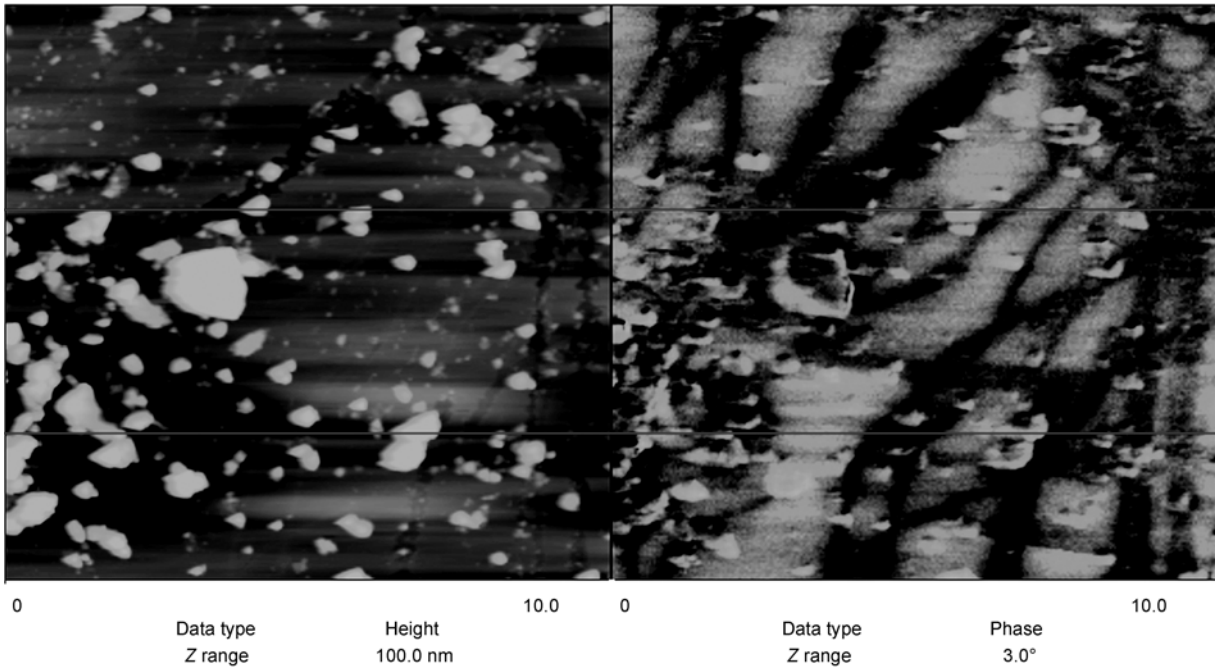


**Figure 3** Surface morphology (left) and phase image (right) of quartz sand.

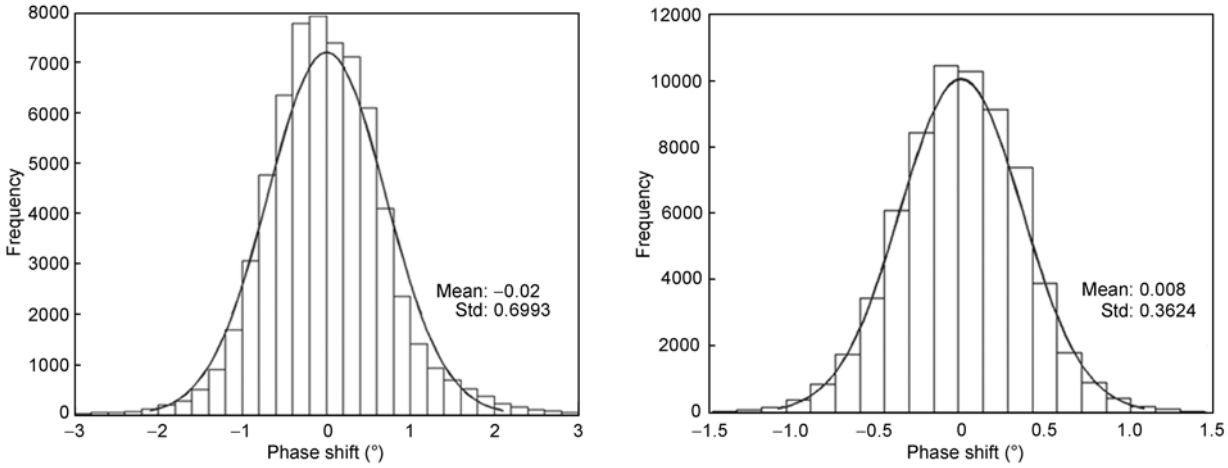


**Figure 4** Frequency histograms of phase shift on quartz sand's surface.

EFM, probe was elevated 50nm vertically and applied voltages of −5, 0 and +5 V in turn. When 0 V was applied, we measured only weak information of charge distribution and phase shift fluctuated within a small area around zero value. When −5 V was applied and sweeping through positively charged regions, tip-sample interaction was attractive, resulting in negative phase shift corresponding to concave parts of the curve; but when sweeping through negatively charged regions, the tip-sample interaction was repulsive, resulting in positive phase shift corresponding to convex parts [18–22]. Similarly, when +5 V was applied, positively charged regions corresponded to convex parts of the curve and negatively charged regions corresponded to concave parts. As can be seen in Figure 6, the concave and convex parts of the curve under voltage of −5 V correspond to convex and concave parts of the curve under voltage of +5V, respectively. So we can acquire the same results of charge distribution for cross sections under either −5 or +5 V bias voltage.

Compared Figure 5 with Figure 6, we can easily find that surface charge distribution has a strong correlation with morphology. Regions with more complex morphology take greater phase shift, which implies greater charge density.

### 3.3 Statistical analysis of charge distribution and morphology

To further analyze the relations between charge distribution

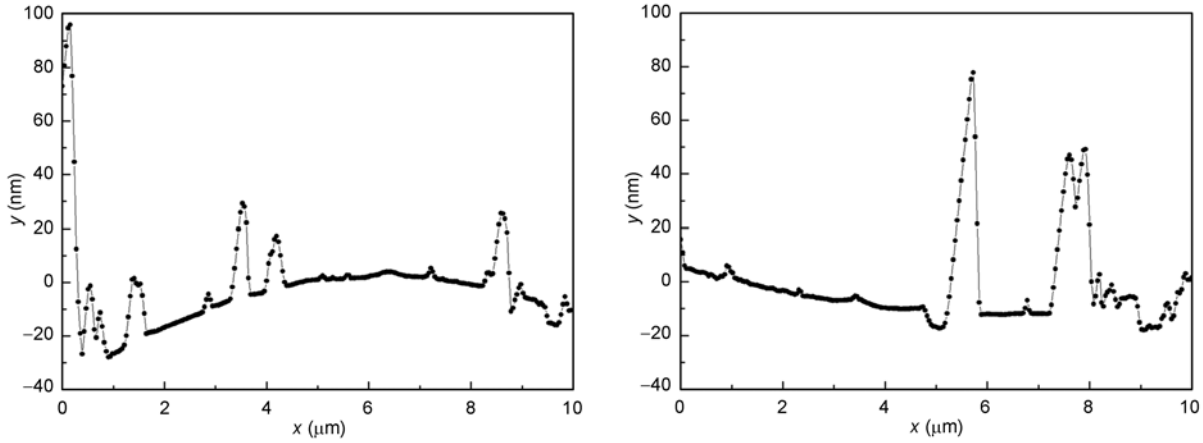


**Figure 5** Morphology images of cross sections corresponding to Figure 3.

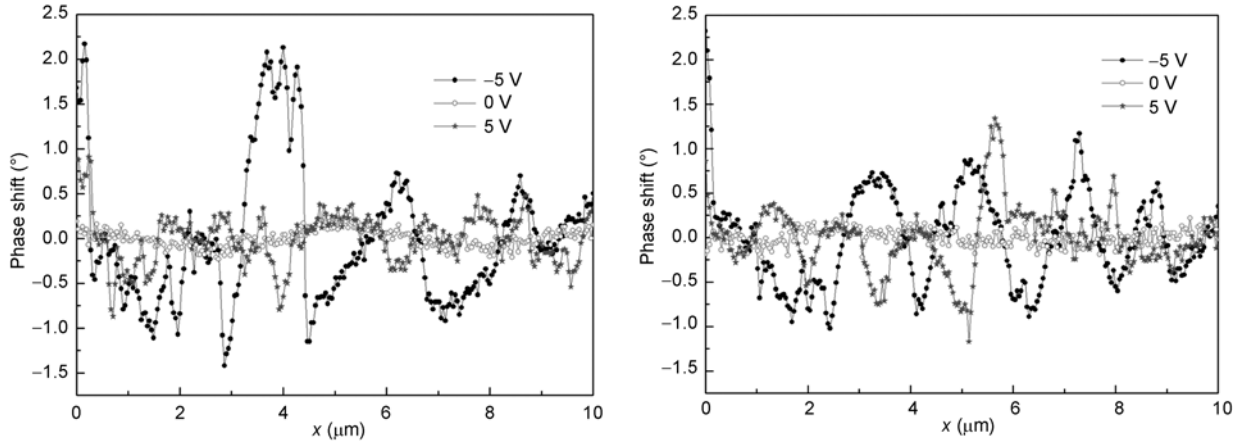


**Figure 6** Phase shifts of cross sections with bias voltages of –5, 0 and 5 V.

and micro-morphology, we conducted a statistical analysis shown in Table 2. Here particle surfaces are classified into concave, convex, groove and ridge, flat and saddle parts by Gaussian curvature $K$ and mean curvature $H$. Table 1 shows the specific classification. Table 2 sorts out the micro-structure of two groups of quartz sands corresponding to charge distribution. Results show that positive and negative charges mostly concentrate on the saddle, convex and concave parts of the surface, with percentages of 53.26%, 22.80% and 22.03%, respectively while distribute less in the groove, ridge and flat parts.

Electrostatic interaction is a major reason for adsorption. Regions with concentrated charge distribution include more active adsorption sites, and adsorb pollutants more easily. Therefore, we can predict that greater adsorption would occur in the saddle, convex and concave parts than in the groove, ridge and flat parts. Chen [23] once did research on the distribution characteristic of adsorbed phosphorus on sediment surface. Spectrum analysis with EDS illustrated phosphorus mostly concentrated on the saddle, convex and concave parts, with percentages of 57.50%, 20.80% and 21.60%, respectively while distributed less in the groove, ridge and flat parts. Chen's study confirmed our former prediction. That is, positive and negative charges mostly concentrate on the saddle, convex and concave parts of the surface, which is contrary to the groove, ridge and flat parts.

Further, we analyzed the relations between surface charge and non-spherical curvature $T$, as seen in Figure 7. Non-spherical curvature is defined as

$$T = \frac{1}{2}\left(C_{\max} - C_{\min}\right).$$

On the surface of sphere, the maximum curvature and minimum curvature are equal, so $T = 0$. A greater non-spherical curvature implies more complex morphology [24]. In Figure 7, $y$-axis represents phase shift, which characterizes the magnitude of surface charge. As the data in Figure 7 were obtained under bias voltage of +5 V, positive and negative phase shifts imply positive and negative charges, respectively. $X$-axis represents non-spherical curvature using logarithmic coordinate. To eliminate the impact of particle size and improve the universality, we normalized the curvature through dividing by the maximum

**Table 1** Classification of particle surface morphologies [22]

| Geometry | Micro-morphology | Gaussian curvature $K$ | Mean curvature $H$ |
|---|---|---|---|
| Elliptic point | Concave | >0 | >0 |
| | Convex | >0 | <0 |
| Parabolic point | Groove | =0 | >0 |
| | Ridge | =0 | <0 |
| Flat point | Flat | =0 | =0 |
| Hyperbolic point | Saddle | <0 | – |

**Table 2** Relations between surface charge distribution and micro-morphology

| Group | | Saddle | Convex | Concave | Groove | Ridge | Flat | Total |
|---|---|---|---|---|---|---|---|---|
| 1# | Number | 31886 | 13229 | 12745 | 106 | 104 | 906 | 58070 |
| | % | 54.91 | 22.78 | 21.95 | 0.18 | 0.18 | 1.56 | 100 |
| 2# | Number | 33959 | 14955 | 14485 | 119 | 133 | 1000 | 64651 |
| | % | 52.53 | 23.13 | 22.40 | 0.18 | 0.21 | 1.55 | 100 |
| Total | Number | 65845 | 28184 | 27230 | 225 | 237 | 1906 | 123627 |
| | % | 53.26 | 22.80 | 22.03 | 0.18 | 0.19 | 1.54 | 100 |

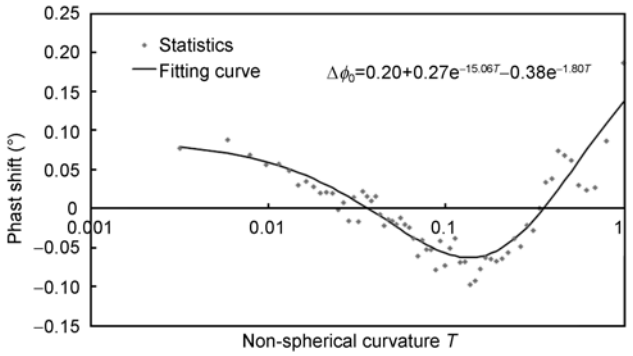


**Figure 7** Relations between surface charge distribution and non-spherical curvature.

value of $T$. The fitting result is as follows:

$$\Delta\phi_0 = 0.20 + 0.27\mathrm{e}^{-15.06T} - 0.38\mathrm{e}^{-1.80T}. \quad (4)$$

Eq. (4) reflects the impact of morphology on charge distribution. Combining with the calculation of non-spherical curvature, we can estimate the charge distribution on particle surface using eq. (4).

It can be seen from Figure 7, when $0.05<T<0.5$, the surface is negatively charged and reaches the extreme near $T$=0.2. When $0<T<0.05$, the surface is positively charged. The smaller non-spherical curvature is, the greater surface charge is, and it tends to a constant gradually. When $0.5<T<1$, the surface is also positively charged. However, the greater non-spherical curvature is, the greater surface charge is, with a relative high growth speed.

## 4 Conclusions

In this paper, we studied charge distribution on the surface of quartz sand with EFM, and obtained the following conclusions.

1) Compared with SEM image, AFM image not only has a high resolution, but also can directly give the surface height of particle, providing convenience for data analysis. SEM image can only provide surface gray value, not real morphology information.

2) Quartz sand particles have extremely complex morphology, which impact charge distribution greatly. Surface charges mostly concentrate on the saddle, convex and concave parts of the surface, with percentages of 53.26%, 22.80% and 22.03%, respectively while distribute less in the groove, ridge and flat parts.

3) Both positively charged and negatively charged regions exist on the surface of quartz sand, with an overall performance of negative charge. Statistics show that surface charge has a good correspondence with non-spherical curvature.

This paper took quartz sand for example to analyze the impact of micro-morphology on charge distribution to provide a foundation for further study of sediment surface nature and the phenomenon of adsorption and flocculation. However, surface morphology of sediment is more complex, which results in difficulties for directly measurement of charge distribution with EFM. So further studies are needed for sediment particles.

*This work was supported by the National Natural Science Foundation of China (Grant No. 50909095) and Chinese Universities Scientific Fund (Grant No. 2011JS131).*

1 Liu D S, An Z S, Wen Q Z, et al. Geological environment of Chinese loess (in Chinese). Chinese Sci Bull, 1978, 23: 1–9

2 Sun Y B, An Z S. Micro-structure and sedimentary characteristics of quartz grains in Eolian deposits (in Chinese). Acta Sedimentologica

Sinica, 2000, 18(4): 506–510
3 Hu Z G, Feng J L, Ju J T. Grain-size distribution and micro-structure of quartz in the Chengdu clay (in Chinese). J Mt Sci, 2010, 28(4): 392–406
4 Ma K J. Morphological study of quartz sand along Zhejiang coast (in Chinese). Donghai Mar Sci, 1991, 9(3): 50–57
5 Ren Z H, Chen D J, Luo Y. Adsorption of amino sulfonate amphoteric surfactants on quartz sand (in Chinese). China Surfactant Detergent & Cosmetics, 2010, 40(6): 410–413
6 Qu C T, Gao X P. Impact of salt on adsorption of thermal recovery additives to quartz sand (in Chinese). J Xi'an Petrol Inst, 1995, 10(4): 50–52
7 Qu C T. Impact of alcohol on adsorption of thermal recovery additives to quartz sand (in Chinese). J Xi'an Petrol Inst, 1995, 10(1): 37–39
8 Wang W W. Experimental study on preparation and $Cu^{2+}$ adsorption capability of ferric salt modified sands (in Chinese). Energ Environ Prot, 2010, 24(4): 20–24
9 Zou W H, Chen Z Z, Han R P, et al. Removal of copper cation and lead cation from aqueous solution by manganese-oxide-coated-sand (in Chinese). Acta Scient Circumst, 2005, 25(6): 779–784
10 Xu G M, Shi Z, Deng J. Characterization of adsorption of antimony and phosphate by using IOCS with XRD, FTIR and XPS (in Chinese). Acta Scient Circumst, 2007, 27(3): 402–407
11 Martin Y, Abraham D W, Wickramasinghe H K. High-resolution capacitance measurement and potentiometry by force microscopy. Appl Phys Lett, 1988, 52: 1103–1105
12 Han L. Nano Fabrication Using Scanning Probe Microscope (in Chinese). Dissertation of Doctoral Degree. Beijing: Tsinghua University, 1999
13 Yang Y Y, Tang H M. Measurement of chitosan material surface charge distribution using scanning probe microscope (in Chinese). J Mat Sci Eng, 2005, 23: 605–608
14 Taboada-Serrano P, Vithayaveroj V, Yiacoumi S, et al. Surface charge heterogeneities measured by AFM. Environ Sci Technol, 2005, 39: 6352–6360
15 Yin X H, Jaroslaw D. Surface charge microscopy: novel technique for mapping charge-mosaic surfaces in electrolyte solutions. Langmuir, 2008, 24 (15): 8013–8020
16 Dianoux R, Martins F, Marchi F, et al. Detection of electrostatic forces with an atomic force microscope: analytical and experimental dynamic force curves in the nonlinear regime. Phys Rev B, 2003, 68: 045403–045408
17 Zhao H B, Han L, Wang X F. A new measurement system based on EFM for charges on dielectric surface in micro-nanometer scale (in Chinese). Insul Mater, 2007, 40: 66–68
18 Zhao H B, Ren Q, Han L. Study on properties of surface charges on polyimide film in micro-nanometer scale (in Chinese). Microf Technol, 2007, 3: 30–33
19 Terris B D, Stern J E, Rugar D, et al. Localized charge force microscopy. J Vac Sci Technol, 1990, A8: 374–377
20 Li Y, Qian J Q, Xu P. Design and research of phase imaging-mode atomic force microscopy (in Chinese). Chin Electr Microsc Soc, 2006, 25: 341–344
21 Magonov S N, Elings V, Whangbo M H. Phase imaging and stiffness in tapping-mode atomic force microscopy. Surf Sci, 1997, 375: L385–L391
22 Fang H W, Chen M H, Chen Z H. Surface Characteristics and Model of Environmental Sediment (in Chinese). Beijing: Science Press, 2009
23 Chen M H. Experiment study on phosphorus adsorption and micro-morphology change of sediment (in Chinese). Dissertation of Doctoral Degree. Beijing: Tsinghua University, 2008
24 Chen Z H. Experiment study on surface morphology and structural properties of sediment after copper ions adsorption (in Chinese). Dissertation of Doctoral Degree. Beijing: Tsinghua University, 2008